Research Article | Vol. 7, No. 10 | 1 Oct 2016 | BIOMEDICAL OPTICS EXPRESS 4034

Biomedical Optics EXPRESS

Wavelength-normalized spectroscopic analysis of *Staphylococcus aureus* and *Pseudomonas aeruginosa* growth rates

SAMANTHA E. MCBIRNEY,[1] KRISTY TRINH,[2] ANNIE WONG-BERINGER,[2] AND ANDREA M. ARMANI[1,3]

[1]*Department of Biomedical Engineering, University of Southern California, 3651 Watt Way, Los Angeles, CA 90089, USA*
[2]*School of Pharmacy, University of Southern California, 1985 Zonal Avenue, CA 90089, USA*
[3]*Mork Family Department of Chemical Engineering and Materials Science, University of Southern California, 3651 Watt Way, Los Angeles, CA 90089, USA*

Abstract: Optical density (OD) measurements are the standard approach used in microbiology for characterizing bacteria concentrations in culture media. OD is based on measuring the optical absorbance of a sample at a single wavelength, and any error will propagate through all calculations, leading to reproducibility issues. Here, we use the conventional OD technique to measure the growth rates of two different species of bacteria, *Pseudomonas aeruginosa* and *Staphylococcus aureus*. The same samples are also analyzed over the entire UV-Vis wavelength spectrum, allowing a distinctly different strategy for data analysis to be performed. Specifically, instead of only analyzing a single wavelength, a multi-wavelength normalization process is implemented. When the OD method is used, the detected signal does not follow the log growth curve. In contrast, the multi-wavelength normalization process minimizes the impact of bacteria byproducts and environmental noise on the signal, thereby accurately quantifying growth rates with high fidelity at low concentrations.

OCIS codes: (300.6550) Spectroscopy, visible; (120.1880) Detection; (170.1530) Cell analysis.

References and links

1. S. M. Ede, L. M. Hafner, and P. M. Fredericks, "Structural changes in the cells of some bacteria during population growth: a Fourier transform infrared-attenuated total reflectance study," Appl. Spectrosc. **58**(3), 317–322 (2004).
2. M. D. Rolfe, C. J. Rice, S. Lucchini, C. Pin, A. Thompson, A. D. S. Cameron, M. Alston, M. F. Stringer, R. P. Betts, J. Baranyi, M. W. Peck, and J. C. D. Hinton, "Lag phase is a distinct growth phase that prepares bacteria for exponential growth and involves transient metal accumulation," J. Bacteriol. **194**(3), 686–701 (2012).
3. K. S. Kim and B. F. Anthony, "Importance of bacterial growth phase in determining minimal bactericidal concentrations of penicillin and methicillin," Antimicrob. Agents Chemother. **19**(6), 1075–1077 (1981).
4. C. B. Black, T. D. Duensing, L. S. Trinkle, and R. T. Dunlay, "Cell-based screening using high-throughput flow cytometry," Assay Drug Dev. Technol. **9**(1), 13–20 (2011).
5. D. K. Button and B. R. Robertson, "Determination of DNA content of aquatic bacteria by flow cytometry," Appl. Environ. Microbiol. **67**(4), 1636–1645 (2001).
6. R. Hazan, Y. A. Que, D. Maura, and L. G. Rahme, "A method for high throughput determination of viable bacteria cell counts in 96-well plates," BMC Microbiol. **12**(1), 259–265 (2012).
7. A. Berrier, M. C. Schaafsma, G. Nonglaton, J. Bergquist, and J. G. Rivas, "Selective detection of bacterial layers with terahertz plasmonic antennas," Biomed. Opt. Express **3**(11), 2937–2949 (2012).
8. K. Hamasha, Q. I. Mohaidat, R. A. Putnam, R. C. Woodman, S. Palchaudhuri, and S. J. Rehse, "Sensitive and specific discrimination of pathogenic and nonpathogenic *Escherichia coli* using Raman spectroscopy-a comparison of two multivariate analysis techniques," Biomed. Opt. Express **4**(4), 481–489 (2013).
9. Y. Jo, J. Jung, M. H. Kim, H. Park, S. J. Kang, and Y. Park, "Label-free identification of individual bacteria using Fourier transform light scattering," Opt. Express **23**(12), 15792–15805 (2015).
10. G. B. Jung, S. W. Nam, S. Choi, G. J. Lee, and H. K. Park, "Evaluation of antibiotic effects on Pseudomonas aeruginosa biofilm using Raman spectroscopy and multivariate analysis," Biomed. Opt. Express **5**(9), 3238–3251 (2014).
11. A. Mazhorova, A. Markov, A. Ng, R. Chinnappan, O. Skorobogata, M. Zourob, and M. Skorobogatiy, "Label-free bacteria detection using evanescent mode of a suspended core terahertz fiber," Opt. Express **20**(5), 5344–5355 (2012).
12. G. Heo, Y. S. Kim, S. H. Chun, and M. J. Seong, "Polarized Raman spectroscopy with differing angles of laser incidence on single-layer graphene," Nanoscale Res. Lett. **10**(1), 45 (2015).

#270487 http://dx.doi.org/10.1364/BOE.7.004034
Journal © 2016 Received 13 Jul 2016; revised 1 Sep 2016; accepted 9 Sep 2016; published 14 Sep 2016

Biomedical Optics EXPRESS

13. Q. Song, X. Pan, H. Wang, K. Zhang, Q. Tan, P. Li, Y. Wan, Y. Wang, X. Xu, M. Lin, X. Wan, F. Song, and L. Dai, "The in-plane anisotropy of WTe_2 investigated by angle-dependent and polarized Raman spectroscopy," Sci. Rep. **6**, 29254 (2016).
14. H. Xiao and S. P. Levine, "Application of computerized differentiation technique to remote-sensing Fourier transform infrared spectrometry for analysis of toxic vapors," Anal. Chem. **65**(17), 2262–2269 (1993).
15. P. Naik and E. J. D'Sa, "Phytoplankton light absorption of cultures and natural samples: comparisons using two spectrophotometers," Opt. Express **20**(5), 4871–4886 (2012).
16. J. A. Myers, B. S. Curtis, and W. R. Curtis, "Improving accuracy of cell and chromophore concentration measurements using optical density," BMC Biophys. **6**(1), 4 (2013).
17. J. Shao, J. Xiang, O. Axner, and C. Ying, "Wavelength-modulated tunable diode-laser absorption spectrometry for real-time monitoring of microbial growth," Appl. Opt. **55**(9), 2339–2345 (2016).
18. E. G. Biesta-Peters, M. W. Reij, H. Joosten, L. G. Gorris, and M. H. Zwietering, "Comparison of two optical-density-based methods and a plate count method for estimation of growth parameters of Bacillus cereus," Appl. Environ. Microbiol. **76**(5), 1399–1405 (2010).
19. M. S. Rappé, S. A. Connon, K. L. Vergin, and S. J. Giovannoni, "Cultivation of the ubiquitous SAR11 marine bacterioplankton clade," Nature **418**(6898), 630–633 (2002).
20. B. A. Dmitriev, F. V. Toukach, O. Holst, E. T. Rietschel, and S. Ehlers, "Tertiary structure of *Staphylococcus aureus* cell wall murein," J. Bacteriol. **186**(21), 7141–7148 (2004).
21. T. Strateva and D. Yordanov, "*Pseudomonas aeruginosa* - a phenomenon of bacterial resistance," J. Med. Microbiol. **58**(9), 1133–1148 (2009).
22. D. S. Blanc, C. Petignat, B. Janin, J. Bille, and P. Francioli, "Frequency and molecular diversity of *Pseudomonas aeruginosa* upon admission and during hospitalization: a prospective epidemiologic study," Clin. Microbiol. Infect. **4**(5), 242–247 (1998).
23. E. B. M. Breidenstein, C. de la Fuente-Núñez, and R. E. W. Hancock, "*Pseudomonas aeruginosa*: all roads lead to resistance," Trends Microbiol. **19**(8), 419–426 (2011).
24. J. C. Pechère and T. Köhler, "Patterns and modes of β-lactam resistance in *Pseudomonas aeruginosa*," Clin. Microbiol. Infect. **5**(Suppl 1), S15–S18 (1999).
25. J. E. McGowan, Jr., "Resistance in nonfermenting gram-negative bacteria: multidrug resistance to the maximum," Am. J. Med. **119**(6 Suppl 1), S29–S70 (2006).
26. R. H. Deurenberg and E. E. Stobberingh, "The evolution of *Staphylococcus aureus*," Infect. Genet. Evol. **8**(6), 747–763 (2008).
27. M. Otto, "*Staphylococcus aureus* toxins," Curr. Opin. Microbiol. **17**, 32–37 (2014).
28. J. A. Lindsay and M. T. G. Holden, "*Staphylococcus aureus*: superbug, super genome?" Trends Microbiol. **12**(8), 378–385 (2004).
29. P. D. Lister, D. J. Wolter, and N. D. Hanson, "Antibacterial-resistant *Pseudomonas aeruginosa*: clinical impact and complex regulation of chromosomally encoded resistance mechanisms," Clin. Microbiol. Rev. **22**(4), 582–610 (2009).
30. F. D. Lowy, "*Staphylococcus aureus* infections," N. Engl. J. Med. **339**(8), 520–532 (1998).
31. R. Masuma, S. Kashima, M. Kurasaki, and T. Okuno, "Effects of UV wavelength on cell damages caused by UV irradiation in PC12 cells," J. Photochem. Photobiol. B **125**, 202–208 (2013).
32. L. G. Harris, S. J. Foster, and R. G. Richards, "An introduction to *Staphylococcus aureus*, and techniques for identifying and quantifying *S. aureus* adhesins in relation to adhesion to biomaterials: review," Eur. Cell. Mater. **4**, 39–60 (2002).
33. G. Domingue, J. W. Costerton, and M. R. W. Brown, "Bacterial doubling time modulates the effects of opsonisation and available iron upon interactions between *Staphylococcus aureus* and human neutrophils," FEMS Immunol. Med. Microbiol. **16**(3-4), 223–228 (1996).
34. I. Williams, F. Paul, D. Lloyd, R. Jepras, I. Critchley, M. Newman, J. Warrack, T. Giokarini, A. J. Hayes, P. F. Randerson, and W. A. Venables, "Flow cytometry and other techniques show that *Staphylococcus aureus* undergoes significant physiological changes in the early stages of surface-attached culture," Microbiology **145**(6), 1325–1333 (1999).
35. J. Qiu, D. Wang, H. Xiang, H. Feng, Y. Jiang, L. Xia, J. Dong, J. Lu, L. Yu, and X. Deng, "Subinhibitory concentrations of thymol reduce enterotoxins A and B and α-hemolysin production in *Staphylococcus aureus* isolates," PLoS One **5**(3), e9736 (2010).
36. J. Goldová, A. Ulrych, K. Hercík, and P. Branny, "A eukaryotic-type signalling system of *Pseudomonas aeruginosa* contributes to oxidative stress resistance, intracellular survival and virulence," BMC Genomics **12**(1), 437 (2011).
37. L. Yang, J. A. J. Haagensen, L. Jelsbak, H. K. Johansen, C. Sternberg, N. Høiby, and S. Molin, "In situ growth rates and biofilm development of *Pseudomonas aeruginosa* populations in chronic lung infections," J. Bacteriol. **190**(8), 2767–2776 (2008).

1. Introduction

Understanding and accurately characterizing the different stages of microbial growth plays a key role in a wide range of fields spanning from therapeutic design and development to diagnostics and disease prevention. Microbial growth is characterized by four distinct phases: lag phase, exponential or log phase, stationary phase, and death phase. The lag phase is considered to be the initial period of slow growth, during which time cells are enlarging and

Biomedical Optics EXPRESS

synthesizing critical proteins and metabolites. This phase is followed by the exponential growth phase, sometimes known as the logarithmic growth phase. During growth, cell division proceeds at a constant rate with the number of cells doubling every unit of time, known as the doubling, or generation, time. Generation times for bacteria vary widely and can range from minutes to days. During the stationary phase, conditions begin to become unfavorable for growth, and bacteria stop replicating. During the death phase, cells lose viability [1–3]. In order to fully map out this process, a measurement method must be able to take readings quickly, iteratively, and reliably over long periods of time. Additionally, the technique should be resistant to potentially confounding signals, such as waste byproducts from the cells and thermal drifts.

As a result of its importance, a wide range of methods have been developed for determining the growth rate, ranging from ultrasensitive flow cytometry to automated counting of bacteria colonies in images. When accuracy is critical, flow cytometry is typically the preferred solution. However, it requires the bacteria to be fluorescently labeled, either through genetic engineering (e.g. GFP, RFP) or with a fluorescent tag [4,5]. In contrast, bacteria colony counting does not have this requirement, but it is significantly less sensitive and is prone to large error values [6]. The importance of these measurements in a wide range of settings from biomanufacturing to basic research has motivated other label-free methods based on spectroscopy to be developed.

The rise in advanced spectroscopy methods has provided a broad toolset for biologists to choose from when performing these analytical measurements. For example, using Raman and FTIR spectroscopy, researchers have monitored the formation of individual bacterium and bacteria layers and the layer response to different antibiotics, enabling rapid optimization of therapeutics [7–11]. However, research has also shown that the results can be strongly dependent on the instrument configuration [12–14]. Additionally, the methods are extremely time-consuming and rely on access to advanced instrumentation. Given the important role that these results play throughout microbiology, a quantitative, reproducible, and rapid technique for determining bacteria concentration in cell media can significantly impact and improve a wide range of applications [15].

In industrial and microbiology lab settings, optical density (OD) measurements have become the preferred approach because of their simplicity and rapid time to answer. Based on optical spectroscopy, an OD measurement characterizes the amount of light that is lost due to scattering and absorption at a single wavelength [16]. In bacteria analysis, 600 nm is frequently used, resulting in the nomenclature OD600. Based on previous work, it is presumed that the OD correlates directly with the cell concentration [17]. Several studies came to the conclusion that OD600 measurements are very reliable and reproducible [18]; however, this conclusion was based on accepting error rates greater 50%. This error can be attributed to many issues that are readily solvable.

For example, it is known that bacteria generate byproducts as they grow. These byproducts can lead to an increase in absorption. Therefore, in addition to the optical loss due to scattering, these byproducts may also contribute to the signal. Additionally, the internal, sub-wavelength components of the bacteria could also contribute to an increase in optical loss. Finally, bacteria are found in a range of morphologies and sizes. Because OD600 measurements are based on the assumption that the scattering signal directly correlates with the concentration, this variation could undermine this relationship. Notably, some bacteria are actually smaller than 600 nm, making them poor-scatterers [19]. Yet, other bacteria will clump or form long chains during growth [20] when a critical concentration is reached, resulting in a non-uniform growth signal. Given the diversity in size, shape, and growth patterns of various bacteria, it would seem advantageous to use a multi-wavelength analysis approach to maximize the accuracy of the signal.

While the OD600 technique is attractive for its simplicity, relying on a single wavelength can significantly increase the impact of these morphological and environmental variations on the detected signal. Therefore, taking into account recent advances in the field of optical spectroscopy and signal analysis, it is critical to rigorously evaluate the efficacy and accuracy

Biomedical Optics EXPRESS

of the current OD600 approach, particularly given previous work demonstrating discrepancies between different spectrophotometers [15]. By conducting full spectrophotometric analyses on samples as opposed to only looking at a single wavelength of light, perhaps it is possible to glean more information on the growth patterns of samples, thereby shedding more light on the different growth stages.

To study this hypothesis, we chose to measure the growth kinetics of *Pseudomonas aeruginosa* and *Staphylococcus aureus*. These two bacteria strains were chosen for the present study for both their similarities and their differences. Their similarities lie in the manner of infection and virulence, while their differences lie in more fundamental aspects; namely, their shape, motility, and growth patterns. *P. aeruginosa* is one of the leading nosocomial pathogens, responsible for 10-15% of nosocomial infections worldwide, and it has joined the rank of "superbugs" due to its resistance to practically all antimicrobial drugs available on the market [21–23]. Additionally, this bacterium is very adaptable, and it is able to continuously develop new resistance mechanisms as new antimicrobial agents are created [21,24,25]. Similarly, *S. aureus* is a dangerous and versatile pathogen that causes a variety of severe diseases; most frequently, skin and respiratory tract infections [26]. *S. aureus* is the most common nosocomial pathogen, and it is associated with high morbidity and mortality, causing clinical disease in 2% of all patient admissions [27,28]. Like *P. aeruginosa*, *S. aureus* is also an extraordinarily adaptable pathogen with a proven ability to develop resistance.

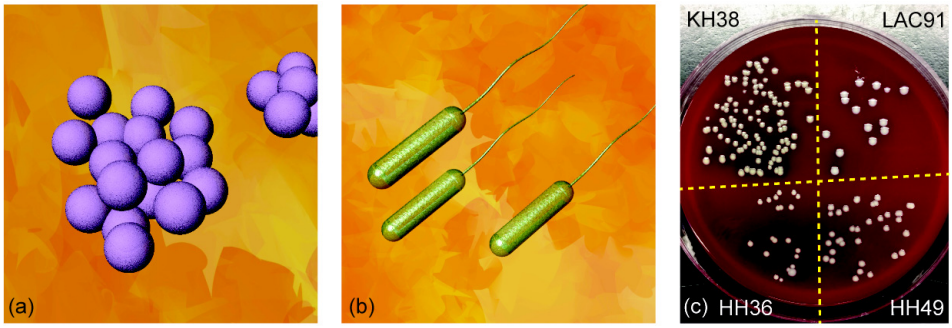

Fig. 1. a) Rendering of *S. aureus*, b) Rendering of *P. aeruginosa*, c) Optical image of four different clinical *S. aureus* strains grown on blood agar plate.

While *P. aeruginosa* and *S. aureus* exhibit many similarities, there are also several key differences between these two bacteria (Fig. 1(a)-1(b)). *P. aeruginosa* is a Gram-negative rod-shaped bacterium, known for growing in isolation from other colonies. Almost all strains are motile by means of a single polar flagellum [29]. *S. aureus* is a Gram-positive, non-motile, small, round-shaped bacteria, typically found growing in grape-like clusters [30]. Characterizing the growth cycles of *P. aeruginosa* and *S. aureus* will lead to a better understanding of the pathogenesis of infections caused by these bacteria. Additionally, these two bacteria provide a rigorous and biologically relevant test of our system, allowing us to verify the universal applicability of the method.

2. Materials and methods

2.1 Preparation of bacterial cultures

Four different clinical strains of *S. aureus* (LAC91, KH38, HH49, and HH36) and one laboratory reference strain of *P. aeruginosa* (PA01) were reconstituted from frozen stock. Clinical strains were obtained directly from patient specimens, whereas laboratory reference strains have been sub-cultured for decades since their first isolation. *P. aeruginosa* (PA01) comes from a strain originally isolated in 1955, and subcultures have been passaged on laboratory media and shared among microbiological laboratories all over the world since. It is important to note that, in the course of sequential *in vitro* passage, laboratory reference strains may have significantly differentiated depending on growth conditions from non-passaged

Biomedical Optics EXPRESS

clinical samples. After lightly scratching the surface of the frozen stock with a sterile inoculating loop, bacterial cultures were suspended in 5 mL tryptic soy broth (TSB) using a vortex mixer and grown in a shaking incubator at 37°C for 24 hours. The culture was kept in a shaking incubator for the duration of the experiments.

2.2 Preparation of bacterial culture dilutions

At the start of the measurements, the cultures were diluted. Two different dilutions were used in the present series of measurements.

To perform the colony counting, the cultures were plated at a 10^{-10} dilution, diluted in tryptic soy broth. This dilution factor was chosen for the purpose of ensuring a representative number of colonies. If there are too many colonies present when plating, counting them is not possible and the numbers are too high to be relevant, while if there are too few colonies, there are not enough for the count to be significant. Additionally, in order for colonies to form visibly, there must be a minimum number of bacteria.

For the OD600 and the multi-wavelength normalization measurements, the level of dilution was 1:40. This dilution was performed in 15-minute intervals, in time with the spectroscopic measurements. At each interval, 50 µL from the overnight culture was added to 1950 µL of fresh sterile tryptic soy broth, resulting in a 1:40 dilution. This concentration was optimized to match the working range of the spectrophotometers used for these measurements (Biochrom WPA Spectrawave S1200 Spectrophotometer and Tecan Magellan Sunrise Spectrophotometer).

2.3 Colony counting

As an alternative to the OD600, colony-counting measurements were also performed. Five hours into the spectroscopy measurements, the bacteria strains were plated to yield an approximate concentration. *S. aureus* strains were plated on blood agar plates. 10 µL was drawn from each 10^{-10} dilution and dropped onto the plate. Using a sterile loop, the bacteria were spread over a section of the plate to create a streak in one quadrant. This procedure was repeated with a fresh sterile loop for each of the subsequent *S. aureus* strains, filling up each of the four quadrants of the blood agar plate. A similar procedure was used to plate the *P. aeruginosa* strain; however, a Pseudomonas Isolation Agar (PIA) plate was used. Plates were incubated overnight at 37°C and colonies counted 24 hours later.

Figure 1(c) shows the optical images of the *S. aureus* bacteria cultures plated at 10^{-10} dilutions. The bacterial concentration for each strain is calculated in colony-forming units per milliliter, the standard method used for obtaining microbial concentrations. To determine this value, the number of colonies present is counted. The number of colonies is then multiplied by the dilution factor and divided by the volume plated, in milliliters. Given that the dilution factor is 10^{-10} and strains were plated at 10 µL (or 10^{-2} mL), we can calculate the concentration in colony-forming units per milliliter by multiplying the number of colonies by 10^{12}. Colony counts for each strain, as shown in Fig. 1(c), were as follows: 113 colonies for KH38, 15 colonies for LAC91, 21 colonies for HH36, and 35 colonies for HH49. Therefore, based on the image and subsequent colony counts, the bacterial concentration is approximately determined to be on the order of 10^{13} - 10^{14} colony-forming units per milliliter for each bacteria strain. However, as can be seen, the size of the different colonies greatly varies, and several of the colonies appear to be merging. Both of these can result in a large error in this value.

2.4 OD600 measurements

OD600 measurements were performed using a Tecan Magellan Sunrise Spectrophotometer. This specific instrument is the standard one used for this measurement in a core facility. All measurements were conducted at room temperature and taken at 15-minute intervals for 11 hours, starting 24 hours after inoculation. At each interval, three separate 150 µL samples were measured, per 1:40 dilution of each strain, yielding three values that were then averaged

Biomedical Optics EXPRESS

to obtain a more representative OD600 measurement. No subsequent data analysis was conducted on these measurements, per the protocol.

2.5 Multi-wavelength differential absorbance spectroscopy

The UV-Vis transmission spectra from the bacterial suspensions were recorded using a Biochrom WPA Spectrawave S1200 Spectrophotometer. We characterized the bacteria over a wavelength range of 350 nm through 800 nm. At wavelengths as short as 250 nm, we would expect to see damage to the cell [31]. Therefore, we did not go shorter than 350 nm, so as to avoid cellular damage. At the start of each measurement interval, a background or normalization spectrum was taken using a sample that only contained the TSB. All spectra were normalized using this spectrum by subtracting the absorbance of the growth media from the absorbance of the cultures for each bacteria strain at each time point.

All measurements were conducted at room temperature and taken at 15-minute intervals for 11 hours, starting 24 hours after inoculation, yielding forty-five data points for each strain. The resulting optical spectra were analyzed two ways: 1) the absorbance at 600 nm was determined, and 2) a multi-wavelength normalization analysis was performed. The absorbance at 600 nm is determined from the UV-Vis absorbance spectra. These values can be directly compared with those from the OD600 system. The multi-wavelength normalization analysis is more complex.

First, every spectrum is converted into a three-point wavelength-averaged spectra. The motivation for this averaging process is related to the wavelength accuracy (+/– 2 nm) and reproducibility (+/– 1 nm) of the UV-Vis system. These values are related to the accuracy and reproducibility of the scanning or moving grating. Because the final goal is a differential measurement, in which sequential measurements are subtracted from each other, the accuracy and reproducibility of the wavelength plays a significant role. The averaging process is very straightforward. If the output of the spectrophotometer at three consecutive wavelengths (λ_1, λ_2, λ_3) has the values A_1, A_2, A_3, then the three-point averaged value is $(A_1 + A_2 + A_3)/3$ at λ_2. This process occurs for every set of three wavelengths, iteratively.

From the three-point averaged spectra, two wavelengths and the associated absorbances are identified: 1) a wavelength that experiences a minimum change in absorbance over time ($\lambda_{\Delta min}$), and 2) a wavelength that experiences a maximum change in absorbance over time ($\lambda_{\Delta max}$). The wavelength that undergoes the maximum change and the minimum change for each bacterium was identified by calculating the total change in absorbance over time ($\alpha_{final} - \alpha_o$), with α_{final} being the final absorbance at time t = 11 hours and α_o being the initial absorbance at time t = 0 hours. The wavelengths that yield the greatest and the least differences in absorbance over time were chosen for subsequent analysis. In the final step, the normalized absorbance is calculated by dividing the two absorbance values $((\Delta\alpha_{max})/ (\Delta\alpha_{min}))$.

3. Results and discussion

Figure 2(a) shows a subset of the forty-five UV-Vis spectra for the *S. aureus* strain HH49 after converting to the three-point wavelength-averaged spectra. As can be observed, some wavelengths experience a greater time-dependent change than other wavelengths.

To more clearly see this behavior, the absorbance values at the six wavelengths indicated by black arrows in Fig. 2(a) are plotted in Fig. 2(b). These specific wavelengths were selected to either have minimum or maximum time-dependent change. Several key points can be made based on these results. First, the change in absorbance at 600 nm actually falls in between these two extremes and, therefore, is not ideal for detection of bacteria growth. Additionally, all of the wavelengths with a large change are below 600 nm. When one considers the size of *S. aureus*, the reason for this dependence becomes evident. *S. aureus* is approximately 600 nm in diameter [32].

It is important to verify that better instrumentation is not responsible for the improved signal at the different wavelengths. To study this parameter, the reading at 600 nm from the UV-Vis is compared to the OD600 measurements. Figure 2(c) plots the 600 nm absorbance values from the spectrophotometer and the OD600 measurements together to show the

Biomedical Optics EXPRESS

comparison. The general trends are nearly identical, as is the total signal change, though there is a constant offset. This constant offset could arise from several different parameters including a wavelength calibration error – for example, if one of the systems was not precisely measuring 600 nm. However, given that it is a constant offset, the results between the two systems are in good agreement.

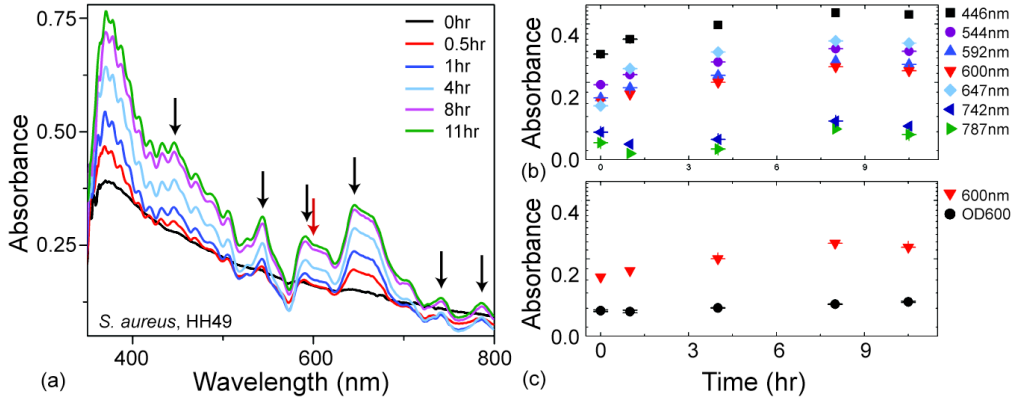

Fig. 2. a) UV-Vis spectra for *S. aureus* strain HH49. Arrows indicate wavelengths chosen for subsequent analysis. b) UV-Vis measurements at wavelengths of interest plotted at select intervals over time. c) OD600 measurements plotted at select intervals over time. Error bars are shown for b) and c); however, the error is so small that the error bars are smaller than the symbols.

Using measurements similar to the ones shown in Fig. 2(a), seven wavelengths were selected for each bacterium based on the same criteria (Fig. 3). For all four of the *S. aureus* strains, the wavelength that undergoes the maximum change is 446 nm, and the wavelength that undergoes the minimum change is 787 nm. Notably, for *P. aeruginosa*, 644 nm changes the most while 600 nm changes the least, yet it is the wavelength used in the typical OD600 measurements. These results were reproduced several times (N = 3), and the ideal wavelengths associated with each bacterium remained constant.

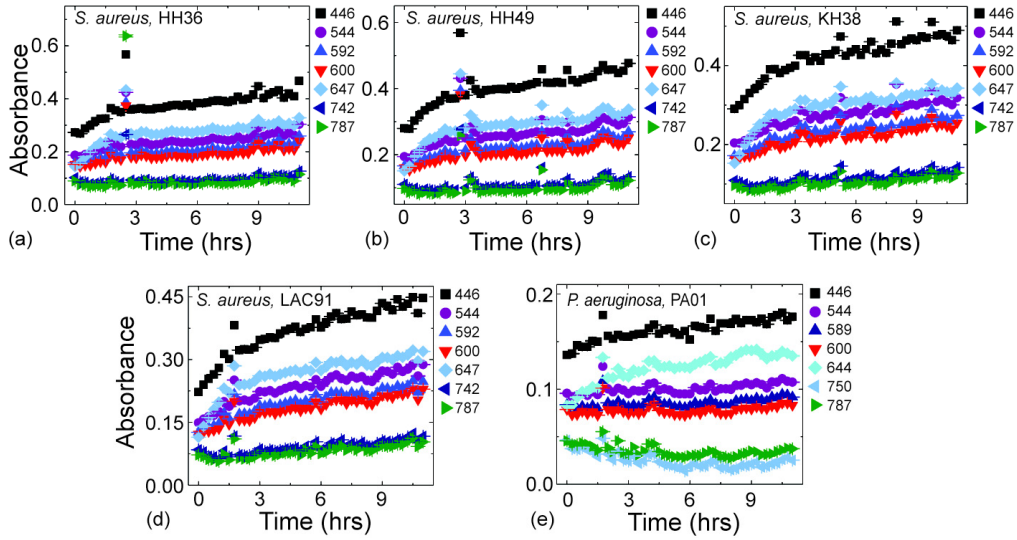

Fig. 3. Change in absorbance over time for seven wavelengths, including 600 nm, exhibiting significant or little change. The specific bacteria plotted are: a) *S. aureus*, HH36 strain, b) *S. aureus*, HH49 strain, c) *S. aureus*, KH38 strain, d) *S. aureus*, LAC91 strain, and e) *P. aeruginosa*, PA01 strain. Error bars are shown on each plot; however, the error is so small that the error bars are smaller than the symbols.

Biomedical Optics EXPRESS

Figure 4 shows the normalized differential absorbance (left axis) and the OD600 measurement (right axis) for each bacterium as a function of time. Several important points become immediately apparent upon analyzing the results. First, while both the wavelength-normalized data and the OD600 data show a general increase in absorbance with time, for the *S. aureus*, the functional form of this increase is completely different (Fig. 4(a)-4(d)). Specifically, for all four strains, the wavelength-normalized data exhibits a well-defined log growth. In contrast, the OD600 shows a somewhat linear and somewhat log trend over the time period studied. It has been well established by different methods that the expected growth curve is logarithmic over this time period [33]. Second, for the case of *P. aeruginosa*, given the noise in the data, the OD600 is unable to detect growth reliably because the noise in the data is larger than the signal, whereas the wavelength-normalized approach easily detects the growth curve with high fidelity (Fig. 4(e)). Therefore, for *P. aeruginosa*, this analysis method is truly an enabling approach.

Using the results shown in Fig. 4, the doubling time for each bacteria strain is calculated. Discarding the lag and stationary phases of growth, we fit the linear portion of the exponential growth curve to a line. The slope of this line is known as μ. Dividing μ into ln(2) yields the doubling time. Doubling times were as follows: 22.42 ± 2.1 minutes for LAC91, 33.44 ± 3.0 minutes for KH38, 37.98 ± 5.4 minutes for HH49, 24.92 ± 1.8 minutes for HH36, and 157.17 ± 19.4 minutes for PA01. *S. aureus* has previously reported doubling times of between 24 and 57 minutes [32–34], while *P. aeruginosa* has reported doubling times of between 100 and 200 minutes [35,36]. Therefore, there is excellent agreement between the current results and previous results in the field. In contrast, the OD600 data taken in parallel is unable to be fit to an exponential function. As a result, it is not possible to calculate doubling times from the OD600 measurements for comparison.

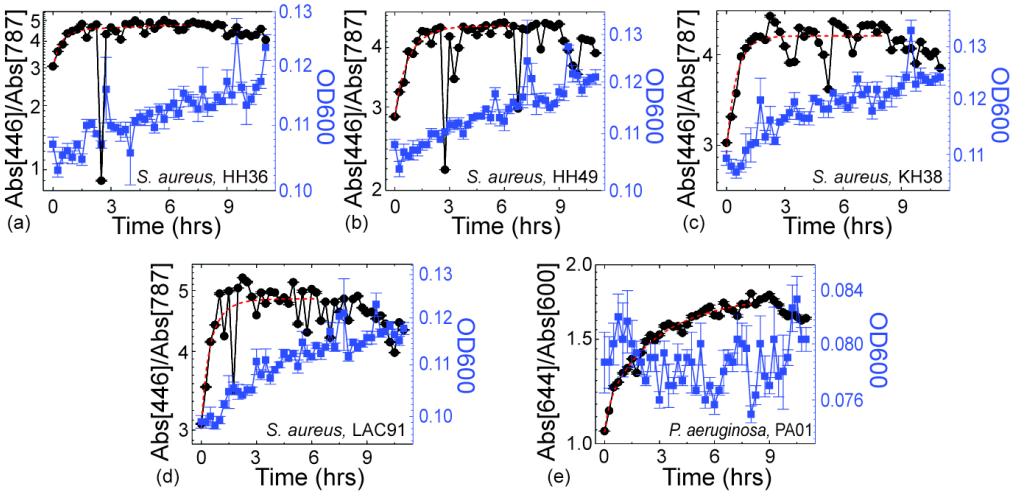

Fig. 4. Wavelength-normalized absorbance and OD600 for each strain plotted as a function of time. The specific bacteria plotted are: a) *S. aureus*, HH36 strain, b) *S. aureus*, HH49 strain, c) *S. aureus*, KH38 strain, d) *S. aureus*, LAC91 strain, and e) *P. aeruginosa*, PA01 strain. Error bars are shown on each plot for both wavelength-normalized absorbance and OD600 measurements; however, the error is so small for the wavelength-normalized absorbance that most of the error bars are smaller than the symbols, while the error is clearly visible for OD600 measurements.

4. Conclusions

The present work proposes and demonstrates that, by implementing a wavelength-normalization step in the data analysis, the accuracy of characterizing the growth rate of a bacteria culture will be significantly improved over the conventional OD600 technique. The proposed method is verified using two distinctly different types of bacteria, *P. aeruginosa* and

Biomedical Optics EXPRESS

S. aureus, and the results obtained are in good agreement with previous values. In contrast, due to poor absorbance at 600 nm, the classic OD600 measurement method is unable to detect the growth rate reliably. Our wavelength-normalization protocol to detect bacteria growth rates can be readily and easily adopted by research labs, given that it only requires the use of a standard spectrophotometer and implementation of a straightforward data analysis method. Measuring and monitoring bacteria growth rates plays a critical role in a wide range of settings, spanning from therapeutic design and development to diagnostics and disease prevention. Having a full understanding of the growth cycles of bacteria known to cause severe infections and diseases will lead to a better understanding of the pathogenesis of these illnesses, leading to better treatment and, ultimately, the development of a cure.

Funding

This work was supported by the Office of Naval Research [N000141410374, N000141110910]. S.E. McBirney was supported by an Alfred Mann Institute Graduate Research Fellowship.